



10-3-3

INFLUENCE OF DISTANCE BETWEEN JUXTAPOSED SHIELD TUNNELS ON THEIR SEISMIC RESPONSES

Yozo GOTO, Takashi MATSUDA, Joji EJIRI and Koji ITO

Technical Research Institute, Ohbayashi Corporation, Tokyo, Japan

SUMMARY

The influence of distance between juxtaposed shield tunnels on their seismic responses was studied by shaking table tests. Two tunnels models, varying the distance between them, were buried in parallel in a sandy ground model, inside a large-sized shearing stack container and were shaken in the perpendicular direction to the tunnel axes. Numerical simulations of the tests were also made by equivalent linear and non-linear FEM. The results obtained are: 1) when the shield tunnels having low rigidity wall approach each other, the section forces of the wall become large, 2) then, it is important to give an appropriate rigidity to the closely constructed shield tunnels.

INTRODUCTION

There are plans in Japan to construct plural numbers of large section shield tunnels juxtaposed in soft ground for use as automobile tunnels of trans-bay highways in building up of metropolitan road systems. However, the influences of earthquakes when shield tunnels lie close to each other have not yet been sufficiently ascertained. And, it is supposed that the interactions between shield tunnels and ground and their stabilities during earthquakes would be greatly influenced by the physical properties of the ground. Therefore, the influences of the distance between tunnels on their response were examined performing large-sized shaking table tests using real ground materials.

SHAKING TABLE TEST

The vibration tests were carried out preparing sandy ground inside a large-sized shearing stack container installed on the shaking table, burying two shield tunnel models in parallel and varying the distance between them. Fig. 1 shows the location of the tunnel models and measuring instruments. The deformation and section force behaviors were observed regarding the excitation direction as perpendicular to the direction of the tunnel axes.

Container and Model Ground The large-sized shearing stack container ($L=4.35\text{m}$, $W=2.85\text{m}$, $H=2.0\text{m}$) has the sidewalls which are horizontally movable in the excitation direction to follow the inside ground behavior. Gifu sand was used as ground material and its physical property is shown in Table 1 and Fig. 2. Gifu sand was spread in several layers inside the stack container and subjected to shaking compaction thoroughly at each time of spread. Physical property of the completed model ground is also shown in Table 1.

Tunnel Model Acrylic made round tubes with diameter $D=50\text{cm}$, overall length $L=150\text{cm}$ and wall thickness $t=1\text{cm}$ were used as tunnels model. Table 2 shows their dimension and physical property. The model tunnel was designed to have smaller stiffness in an attempt to improve the accuracy of measurement and the clearness of phenomenon. Upon examination of the model using the similitude proposed by Kagawa (Ref. 1), it is found that the bending and axial stiffness of the model are as small as $1/15$ and $1/5$ respectively, under the assumption of the prototype tunnel being a large-section one of more than 10m diameter with only primary lining. In the experiment, Gifu sand was pasted around the tunnel models aiming at simulating contact conditions between tunnel and ground as close as possible to the reality.

Arrangement of Instruments Accelerometers were installed in the vertical direction for between-tunnels ground (AC 1-7) and not-between-tunnels ground (AN 1-9). Strain gauges were applied in pairs on the exterior and the interior of the tunnel model at 8 measuring points (STC 1-8) with 45° angle distance apart each other starting from the top of tunnel.

Cases of Experiments The representative experiments were the resonance tests on the following 5 cases; Single and Juxtaposed $0.5D$ (half of diameter), $1D$ and $2D$ with the acceleration of the shaking table kept constant at 80 gals. The thickness of the overburden soil was assumed to be $1D$ in each case.

NUMERICAL ANALYSIS

Analyses were performed using equivalent linear FEM (FLUSH) and non-linear FEM (7S-II) with joint elements and elasto-plastic elements. Two cases $0.5D$ and $2D$ were concerned. The finite element modeling is shown in Fig. 3. The relationships between shear modulus G , damping factor h and shear strain γ used in these analyses were determined applying the dynamic BACK ANALYSIS method (ref. 2) to the results of the resonance tests of the model ground without tunnels.

RESULTS

Fig. 4 shows the resonance curves of section forces of tunnel measured at the point STC 2. At this point, it is found that both bending moment and axial force are apt to increase moderately as the distance between tunnels becomes smaller. This can be explained from Fig. 5, which shows the resonance curve of shear strain in the intermediate ground between tunnels. In other words, the closer the tunnels are constructed to each other, the greater the ground shear strain between tunnels grows, consequently resulting in greater deformation of the tunnels. This is because the increase of the shear strain is attributable to the fact that the deformation in the adjacent ground of the tunnel with low stiffness is intensified as the distance between tunnels gets closer and multiplied with addition of the effect of the dependence of the strain dependent ground stiffness.

Fig. 6 shows the resonance curves at the point STC 8. The point STC 8 revealed the same trend in bending moment as STC 2 but differs in axial force, which becomes smaller as the distance between tunnels closer. The reason is that there may have been slip between the tunnel and ground near this measuring point. This can be ascertained by the analysis performed focusing on the slip between tunnel and ground (7S-II), showing that point around STC 8 causes slip more easily than that around STC 2.

Fig. 7 shows a comparison between the experiment and analytical results measured around the resonance point (9.5Hz) concerning the distribution of section force along the circumferential direction of the tunnel. The overall patterns of the experiment and analysis are well coincident each other. The points STC 2, 4, 6 and 8 show greater section forces than the other measuring points. This can be reasoned as that the tunnel

suffered egg-like shear deformation. With regard to the magnitude of the section forces, the bending moment was found larger in the experiment than in the analysis whereas the axial force was the converse of this. This seems to be attributable to the aforementioned slip between the tunnel and ground.

Fig. 8 describes the shear strain distribution in the vertical direction measured at locations between tunnels, as well as the exterior ground. Of the above locations, the exterior ground shows no difference and likewise the experiment and analytical results are very much coincident. Meanwhile, the ground between the tunnels shows a rapid increase in the shear strain at the location as the same depth as the tunnel. Taking into account that the experimental result represents the averaged value between the two measuring points, it can be said that both experiment and analytical results are well coincidence.

Fig. 9 shows the results of numerical experiment which simulated the response of the model tunnel having the equivalent stiffness of prototype tunnel. The evident influence of distance can not be seen. This implies the importance to design tunnel wall to have sufficient stiffness in the case of the small distance.

CONCLUSIONS

- (1) Dynamic interaction between two tunnels does not have predominant effect on their seismic response.
- (2) When the shield tunnels having low rigidity as composed of only thin segment structures approach each other, there appear regions where large shearing deformations easily occur on the surrounding ground of the tunnel as shown in Fig. 10. Its shearing strain might increase moreover due to the strain-dependent non-linear nature of soil.
- (3) It is important to give an appropriate rigidity to the closely constructed large-section shield tunnels. In reality, tunnels are in general provided with a secondary lining and have greater stiffness than that of the tunnel model herein discussed.
- (4) It is necessary to perform analysis in the aseismic design of actual tunnels into account sliding between ground and tunnels for realization of rational design.

ACKNOWLEDGEMENTS

In the analysis with respect to sliding between tunnel and surrounding ground, we have employed 7S-II developed by the Quake-proof Foundation Department of the Disaster Prevention Research Institute of Kyoto University and we would like to hereby take the opportunity to express gratitude for the above.

REFERENCES

- 1 Kagawa, T., On the Similitude in Model Vibration Tests of Earth-Structures, Proc. of Japan Society of Civil Engineers, No.275, 69-77, (1978), (in Japanese)
- 2 Matsuda, T., Goto Y., Studies on Experimental Technique of Shaking Table Test for Geotechnical Problems, Proceedings of the Ninth World Conference of Earthquake Engineering, (will be published in 1988)

Table 1 Physical Properties of Sand and Model Ground

GIFU SAND	Mean Grain Size (D_{50})	0.33mm
	Specific Gravity (G_s)	2.65
	Max Void Ratio (e_{max})	1.17
	Min Void Ratio (e_{min})	0.74
GROUND	Unit Weight (γ_s)	1.47tf/m ³
	Relative Density (D_r)	86 %
	Mean Shear Velocity (V_s)	130m/sec
	Mean Shear Modulus (G)	2500tf/m ²
	Void Ratio (e)	0.80

Table 2 Mechanical Properties of Shield Model

Material	acryl
Dimensions	$\phi 50 \times L 150 \times t 1 \text{ cm}$
Young's Modulus (E)	30,000 kgf/cm ²
Unit Weight (γ_a)	1.19 tf/m ³
Poisson's ratio (ν)	0.3

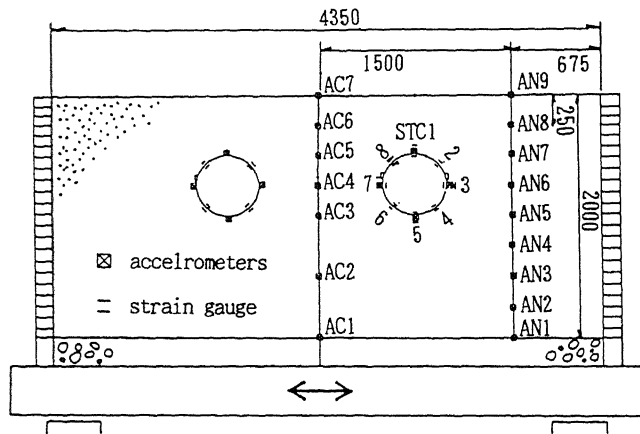


Fig. 1 Measuring Instruments

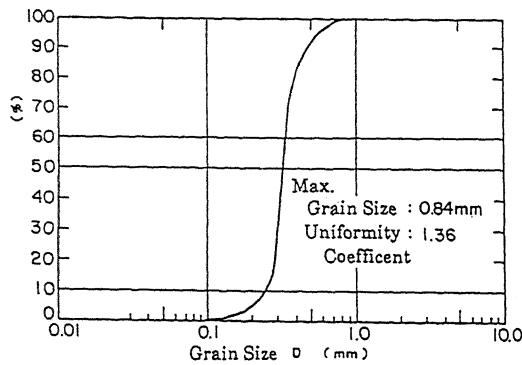
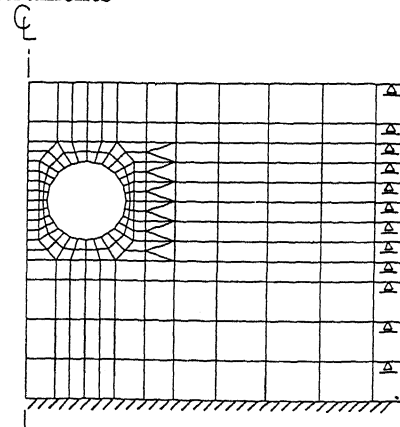


Fig. 2 Grain Size of Gifu Sand



Finite Element Model 0.5D
Fig. 3 Finite Element Model

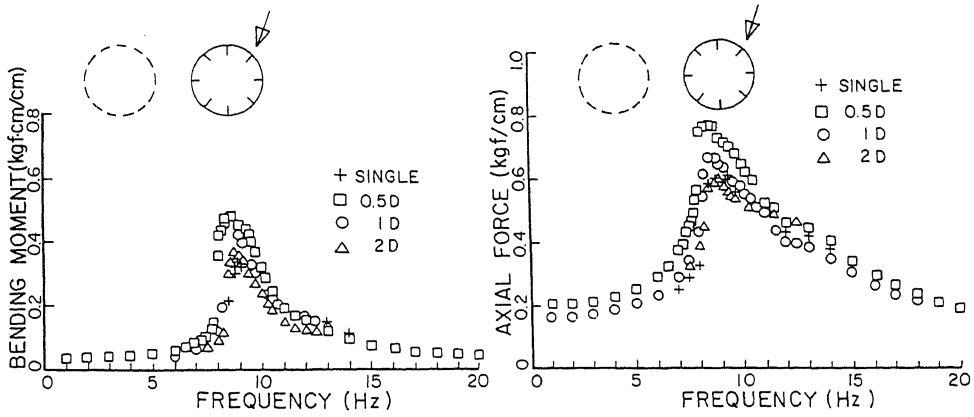


Fig. 4 Resonance Curves of Section Forces at STC 2 (80gals)

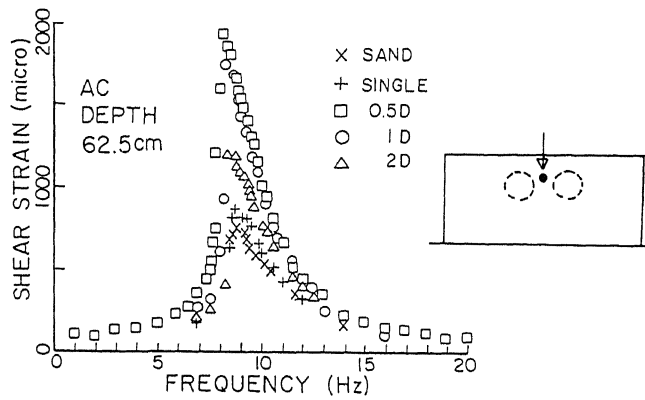


Fig. 5 Resonance Curves of Ground Shear Strain between Tunnels (80gals)

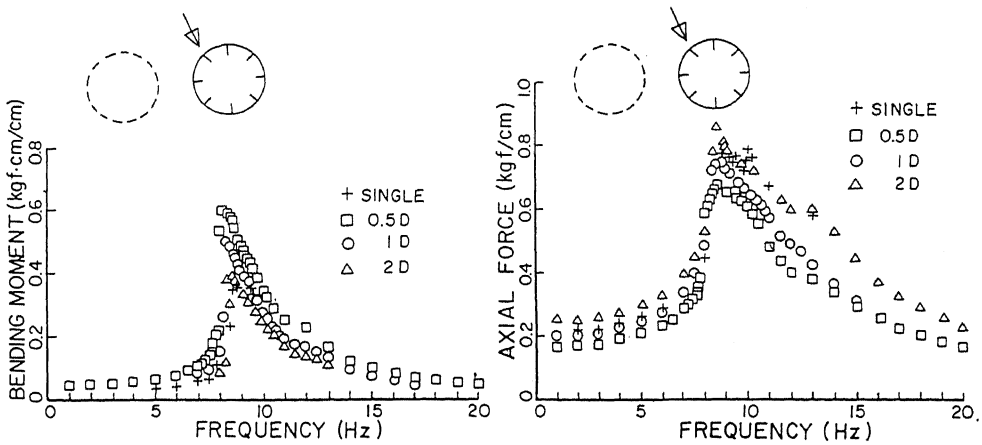


Fig. 6 Resonance Curves of Section Forces at STC 8 (80gals)

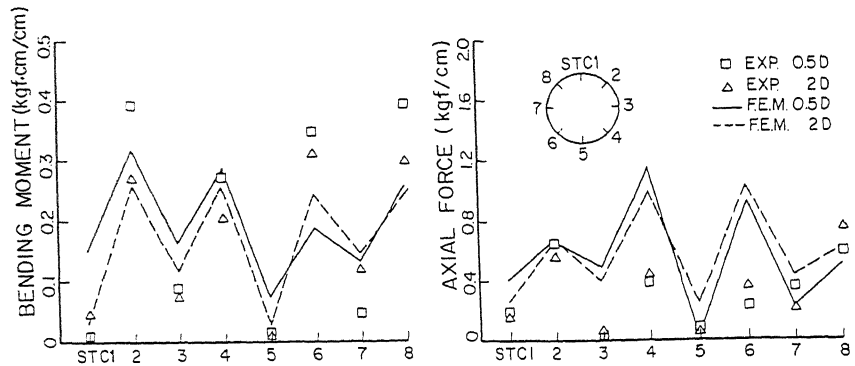


Fig. 7 Circumferential Distribution of Section Forces (9.5Hz, 80gal)

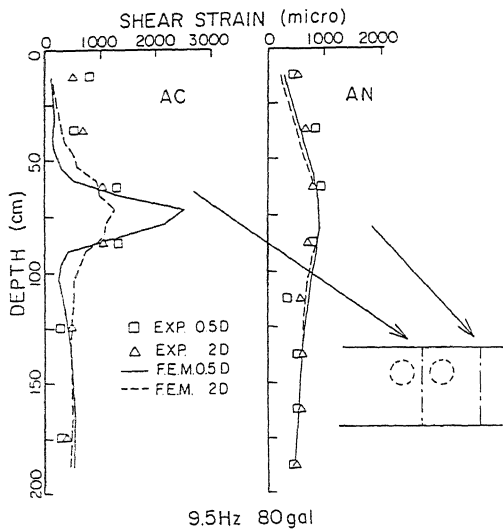


Fig. 8 Vertical Distribution of Ground Shear Strain

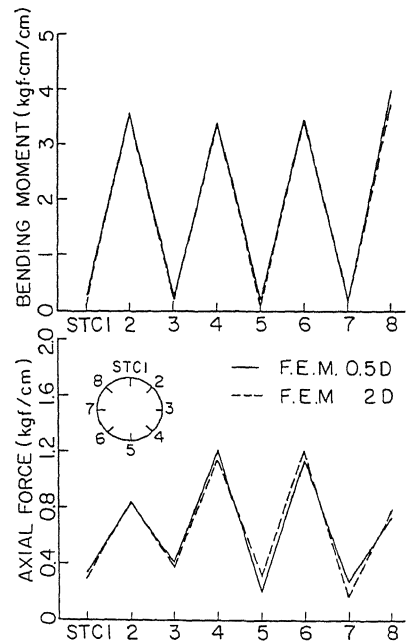


Fig. 9 Circumferential Distribution of Section Forces (9.5Hz, 80gal) in case of Higher Rigidity Tunnel

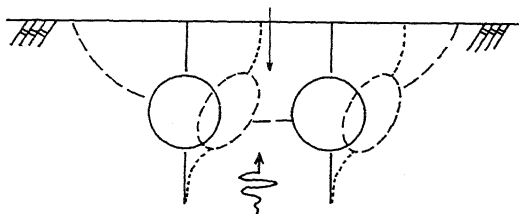


Fig. 10 Large Shearing Deformation Region